

Fluorescence Intermittency in Single InP Quantum Dots

Masaru Kuno,[†] David P. Fromm,^{†,‡} Alan Gallagher,[†] David J. Nesbitt,^{*,†,‡}
Olga I. Micic,[§] and Arthur J. Nozik^{‡,§}

*JILA, National Institute of Standards and Technology and University of Colorado;
Department of Chemistry and Biochemistry, University of Colorado, CB 440,
Boulder, Colorado 80309-0440 and National Renewable Energy Laboratory,
1617 Cole Boulevard, Golden, Colorado 80401*

Received June 25, 2001; Revised Manuscript Received August 9, 2001

ABSTRACT

Fluorescence “blinking” kinetics of isolated colloidal InP quantum dots (QDs) are investigated via confocal single molecule microscopy. Analysis of fluorescence trajectories reveals inverse power law behavior ($\propto 1/\tau^m$) in on/off time probability densities with $m_{\text{on}} \approx 2.0(2)$ and $m_{\text{off}} \approx 1.5(1)$. Such an inverse power law in both on/off times is inconsistent with a static distribution of electron/hole trapping sites and highlights the role of fluctuations in the QD nanoenvironment.

I. Introduction

The new and rapidly evolving area of nanoscience is a fascinating amalgam of different scientific disciplines touching upon traditional areas such as physics, chemistry, biology, and engineering. From a physics perspective, interest in small-scale objects is motivated by the fact that matter in the nanometer size regime can exhibit novel optical/electrical properties that are distinctly different from bulk behavior. Furthermore, chemical phenomena can be profoundly influenced by changes in the “local” molecular environment, stimulating interest in kinetic studies on nanometer length scales. The recent development of single molecule optical techniques addresses both these needs by opening up a powerful set of new experimental tools for studying the kinetics/dynamics of isolated species. In this respect, single-molecule optical studies offer a unique window into the nanosciences, since a number of phenomena such as fluorescence intermittency, spectral diffusion, and charge blinking have been postulated to be sensitive to the “nanoenvironment” of the species under investigation.

This letter describes recent studies of fluorescence kinetics in isolated III–V InP semiconductor quantum dots (QDs), extending and complementing our previous fluorescence studies of II–VI semiconductor CdSe/ZnS QDs. In particular, the present focus is on first observations of so-called fluorescence intermittency effects in colloidal InP QDs, where the fluorescence efficiency of a single, continuously

excited QD modulates rapidly between “on” and “off” levels. Such “blinking” behavior, where the emission of a quantum dot undergoes abrupt and reversible transitions between emitting and nonemitting configurations of the system, appears to be a rather general phenomenon of single-particle microscopy, as witnessed by the observation of such intermittency in fluorescent proteins,¹ light harvesting complexes,² single polymer strands,³ porous silicon,⁴ self-assembled quantum dots,^{5,6} colloidal QDs,^{7–12} single ions,^{13,14} and even single laser dye molecules.^{15–17}

Blinking has been widely attributed to “quantum jump” phenomena first described by Bohr in 1913 and later by Cook and Kimble¹⁸ in 1985. Quantum jumps refer to interruptions of rapid fluorescence cycling inside an “on” manifold of states by infrequent transitions to/from a nonemissive “off” manifold, where the time dependent fluorescence “trajectory” can be used to follow the quantum state evolution of the system. Sustained periods of emission (“ τ_{on} ”), for example, might correspond to fluorescence cycling between optically coupled ground and excited states, with intervening periods of darkness (“ τ_{off} ”) indicating projection of the wave function into an optically “dark” state (e.g., a triplet state), from which it eventually recovers. As generally true in single-particle kinetic studies, the rates for transformation between emitting/nonemitting configurations cannot be obtained in any single measurement, but instead must be statistically inferred via the probability density of on/off times, i.e., $P(\tau_{\text{on}})$ and $P(\tau_{\text{off}})$. For example, the simplest two-level kinetic analysis for interconversion between the two distinct on or off manifold of states predicts a single-exponential decay for $P(\tau_{\text{on}})$ and $P(\tau_{\text{off}})$ as a function of τ_{on} and τ_{off} , from which one can

[†] JILA, National Institute of Standards and Technology and University of Colorado at Boulder.

[‡] University of Colorado, Department of Chemistry and Biochemistry.

[§] National Renewable Energy Laboratory.

readily extract the characteristic forward and reverse rate constants. This quantum jump analysis has been used successfully in the case of single ions confined to radio frequency traps,¹⁹ single molecules at liquid helium temperatures²⁰ and isolated impurities embedded in a crystalline matrix,²¹ revealing intersystem crossing (ISC) rates and dark triplet lifetimes of isolated species. However, application of this kinetic analysis has not been straightforward in many condensed phase fluorescence systems at room temperature, which often do not exhibit single exponential on-time and off-time probability densities. Rather, it is more often the case that both $P(\tau_{\text{on}})$ and $P(\tau_{\text{off}})$ exhibit significantly non-exponential behavior, which renders the simple two-level quantum jump analysis inadequate and requires a more sophisticated kinetic model.

Fluorescence intermittency kinetics of individual ZnS overcoated CdSe QDs has been especially well studied, and serves as a particularly good example of highly multiexponential kinetics. Specifically, instead of single-exponential behavior, the blinking kinetics of individual CdSe QDs has been shown to follow an inverse power law

$$P(\tau) \propto (1/\tau)^m \quad (1)$$

in both $P(\tau_{\text{on}})$ and $P(\tau_{\text{off}})$,^{10,11,22} with the power law exponents of order $m \approx 1.6$. This surprising result has been tested over a remarkable 9 orders of magnitude in probability density and 5 orders of magnitude in time. Stated in the context of a quantum jump model, this would require forward/reverse rate constants to vary dramatically in time from one blinking event to another by as much as 10^5 -fold. These experiments pose the dynamically interesting question: what could be the cause for such large variations in charge-transfer rates characterizing the duration of on/off fluorescence episodes in an isolated QD species?

Previous studies in CdSe/ZnS QDs have begun to identify the critical role of environmental fluctuations in this blinking phenomenon. One widely invoked mechanism for blinking involves electron (or hole) charge transfer between the QD core and a manifold of nearby trap sites, resulting in strong electric fields responsible for increased phonon coupling and reduced fluorescence efficiency. In the context of such a QD ionization model, this 10^5 ratio reflects a similar range of electron/hole transfer rates to/from the QD. As one possible model, for example, this fluorescence intermittency could be rationalized in terms of modest fluctuations in the tunneling barrier height and/or width between the QD and defect states extrinsic to the particle.^{10,11} Physically, this could originate from conformational fluctuations of organic ligands on the surface of the QD, which modulate the effective molecular conductivity of the nanocrystallite relative to states on the substrate or surrounding matrix. Alternatively, this could be due to small spatial displacements of a very small number of donor/acceptor-like states in the surrounding substrate/matrix, which alter the tunneling probability of electrons or holes leaving the nanoparticle. To test models of fluorescence intermittency, however, it would be useful

to have additional kinetic studies of power law blinking in other systems, such as QDs grown alternatively from III–V semiconductor materials.

To address this need, we have extended these single-molecule fluorescence experiments toward colloidal InP semiconductor quantum dots, which serve as the primary focus of this paper. This work represents the first investigation of fluorescence blinking in isolated colloidal InP QDs, and permits direct comparison with extensive blinking kinetic data from other laboratories on colloidal ZnS overcoated CdSe QDs. An outline of the paper is as follows. In section II, we briefly describe experimental details of the single-molecule confocal optical microscope and synthesis of colloidal InP QDs. Experimental data for InP QD fluorescence intermittency is then described in section III, followed by analysis/discussion of these results in section IV. One goal will be to test for the presence of power law kinetics in the InP QD data, as well as consistency with simple dynamical models of carrier tunneling through fluctuating barriers. The conclusions of the work are summarized in section V.

II. Experiment

The experiments are conducted using a confocal optical microscope in an epi-illumination configuration. The excitation source is the amplitude-stabilized 488 nm line of an air cooled Ar⁺ laser that has been optically filtered to eliminate contamination by other laser lines and residual plasma light. Samples consist of very dilute solutions ($\approx 10^{-10}$ M) of colloidal InP quantum dots dispersed in hexanes spin coated onto a glass coverslip that has been flamed with an acetylene torch to remove fluorescent impurities. A computer-controlled x, y, z piezo stage scans the coverslip sample under a diffraction limited laser excitation spot, with sample emission collected through the same air (0.9 NA) or oil immersion (1.4 NA) objective to generate a $10 \mu\text{m}$ by $10 \mu\text{m}$ (265×256 pixel), two-dimensional (2D) image. The emission is filtered with a holographic notch/colored glass filter combination to remove any residual 488 nm light and imaged onto an avalanche photodiode (APD). Displacements of the piezo stage with voltage are calibrated interferometrically with the 632.8 nm line of a HeNe laser. To isolate the fluorescence from an individual QD, the stage is piezoelectrically adjusted to maximize emission from a single particle. Time dependent fluorescence “trajectories” are then taken with a multichannel scaler with typical integration times of 10 ms. To quantify the fluorescence detection process, we have determined the total collection efficiency of the confocal apparatus (i.e., APD photoelectrons detected per fluorescence photon emitted), based on isotropic light scattering from a BaSO₄-coated substrate.^{10,11} The results indicate 0.87 (1)% and 5.61 (8)% for a dry 0.9 NA and 1.4 NA oil immersion objective, respectively. These collection efficiencies have also been tested against single dye molecule fluorescence studies, based on previously measured quantum yields (≈ 0.80) and absorption cross sections ($\approx 1.32 \times 10^{-16}$ cm²) for R6G coated on surfaces. These single R6G molecule fluorescence

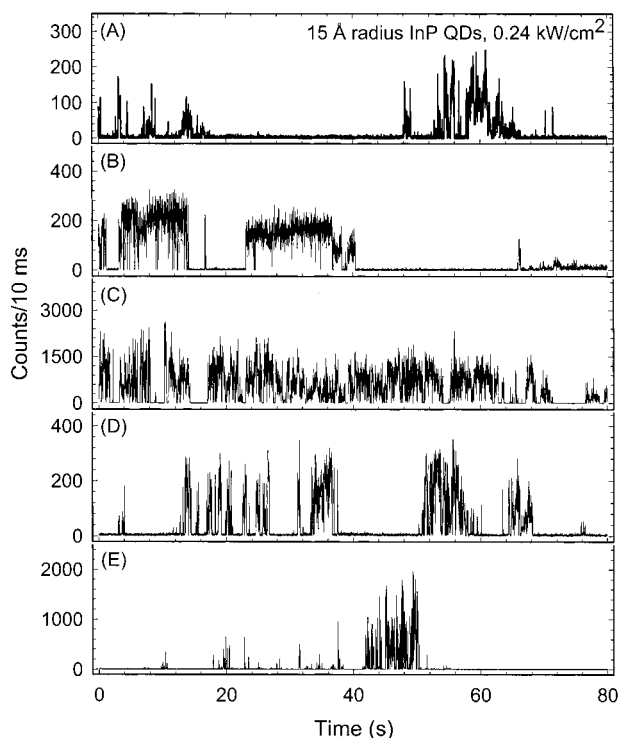


Figure 1. Fluorescence trajectory of five isolated (15 Å radius, HF etched) InP QDs dispersed on a glass coverslip. The excitation intensity is 0.24 kW/cm² and the integration time is 10 ms/bin in all cases.

results yield 0.8 (9)% and 3.4 (3)% for the NA = 0.9 and 1.4 objectives, which is in reasonable agreement with the BaSO₄ light scattering measurements.

The InP QDs used in this study are made by the decomposition of indium oxalate and (trimethylsilyl)phosphine in a hot coordinating solvent (trioctylphosphine oxide, TOPO and trioctylphosphine, TOP) over the course of several days. The high temperatures (250–300 °C) ensure a highly crystalline (zinc blende) product with a surface passivated with TOPO/TOP. The synthesis is then followed by etching the InP nanocrystallites in a dilute butanolic solution of HF or NH₄F, which suppresses any deep trap emission thought to originate from surface defects and improves the band edge emission quantum yield. The etched particles are finally exposed to octanethiol, which passivates the HF treated surface. This surface passivation procedure significantly improves the fluorescence properties of colloidal InP quantum dots, similar in spirit to “overcoating” methods recently developed to improve the quantum yield of CdSe QDs.^{23–26}

III. Results

Figure 1 shows fluorescence trajectories of five 15-Å-radius InP QDs isolated on the surface of a glass microscope coverslip, selected arbitrarily from the larger set of 33 InP QDs that we have investigated. The trajectories clearly reveal blinking dynamics, with the fluorescence counts per 10 ms integration time window turning on and off abruptly, despite continuous laser excitation at an intensity of 0.24 kW/cm².

These data represent the first such evidence for blinking behavior in single colloidal InP QDs, although such behavior has been seen in MOCVD grown InP QDs^{5,6} and is consistent with the blinking dynamics more extensively investigated in CdSe/ZnS QDs. Also evident are strong qualitative differences in the nature of fluorescence episodes for different dots as well as laser intensities. For example, some trajectories exhibit “digital” behavior (e.g., panel B) with sustained on periods, versus much more chaotic behavior (e.g., panels A and E) with τ_{on} durations down to the 10 ms integration time window limit, i.e., qualitatively similar to previous reports of CdSe/ZnS QD blinking dynamics. This dependence on laser intensity is reasonable; the on \rightarrow off rates for InP QDs scale with higher excitation intensities, thereby shortening the on time distribution. From this perspective, chaotic trajectories simply reflect when the on time distribution becomes comparable to (or smaller than) the data integration window, which results in averaging multiple on/off transitions per time bin. Conversely, at lower excitation intensities this time scale becomes much longer, and digital trajectories are more common. A more detailed analysis of such fluorescence dynamics in digital and chaotic regimes can be satisfactorily reproduced from simple kinetic models and will be discussed elsewhere.

From a more mathematically rigorous perspective, the blinking kinetics of these InP QDs can be quantified by analysis of the on-time and off-time probability densities, $P(\tau_{\text{on}})$ and $P(\tau_{\text{off}})$. We obtain these probability densities from individual InP fluorescence trajectories by defining an on/off intensity threshold, typically set to twice the background APD level. These statistics are collected over the entire fluorescence trajectory of a single QD to generate raw histograms of on-times (τ_{on}) and off-times (τ_{off}), which directly reflect the number of occurrences of a particular τ_{on} or τ_{off} value. At sufficiently long times, however, these histograms have only one or no counts per time bin due to finite counting statistics. Therefore, the most appropriate continuous on-time/off-time probability densities [$P(\tau_{\text{on}})$ and $P(\tau_{\text{off}})$] are obtained by weighting each point in the on/off histograms by the average time between nearest neighbor event bins. This does not impact data at short event durations due to the presence of counts in each time bin; however, it does correct for finite statistics at long times. This weighting procedure therefore ensures that the modified $P(\tau_{\text{off}})$ and $P(\tau_{\text{on}})$ distributions remain smooth in this long on-time/off-time region, providing the statistically best estimates of the true on-time and off-time probability densities.

The exponential vs nonexponential character of $P(\tau_{\text{on}})$ and $P(\tau_{\text{off}})$ density can be tested by semilogarithmic plots shown in Figure 2 (A,C). Physically, linear semilogarithmic plots in either $P(\tau_{\text{on}})$ or $P(\tau_{\text{off}})$ vs time would indicate the existence of a characteristic rate constant for either the (on \rightarrow off) or (off \rightarrow on) transition. However, this is decidedly not the case; strong curvature is observed in semilogarithmic plots of both on-time and off-time probability densities. This manifests itself as nonexponentiality over a large dynamic range of times; the insets in Figure 2 represent the first 0.5 s enlargements of the graph showing curvature even on the shortest

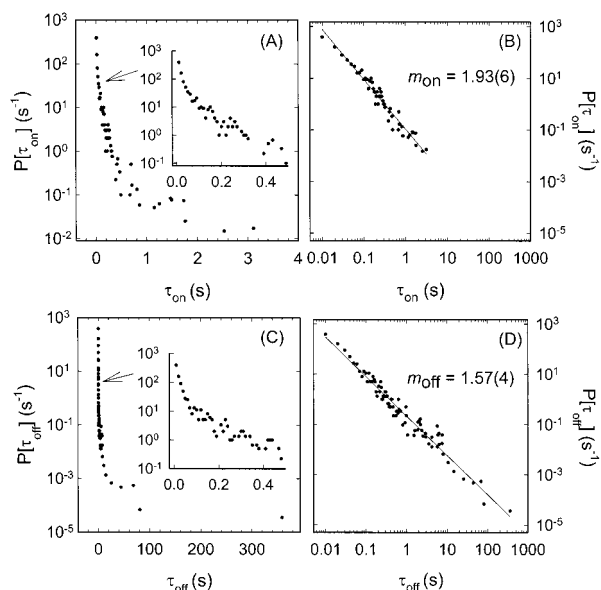


Figure 2. (A) Semilogarithmic plot of the on-time probability density $[P(\tau_{\text{on}})]$ for a single InP quantum dot. The inset shows the first 0.5 s of data. (B) log-log plot of $P(\tau_{\text{on}})$ versus time. (C) Semilogarithmic plot of the off-time probability density $[P(\tau_{\text{off}})]$ for the same QD. The inset is again an enlargement of the first 0.5 s of data. (D) log-log plot of $P(\tau_{\text{off}})$ versus time. Linearity in log-log plots of $P(\tau_{\text{on/off}})$ vs $\tau_{\text{on/off}}$ represent the unambiguous signature of inverse power law kinetics.

time scales experimentally monitored. Furthermore, all InP QDs investigated exhibit such multiexponentiality in their blinking kinetics, irrespective of size (15 to 54 Å) and excitation intensity (100 to 400 nW).

In light of the power law kinetics previously observed for CdSe/ZnS QDs, log-log plots provide a more quantitatively useful representation of this on/off statistical data. These data are shown in Figure 2 (B,D) and reveal remarkably linear behavior characteristic of an inverse power law $[P(\tau_{\text{on/off}}) \propto 1/\{\tau_{\text{on/off}}^m\}]$.^{10,11,22} This observation is consistent with results obtained from CdSe QDs showing the existence of highly nonexponential, inverse power law behavior in both $P(\tau_{\text{on}})$ and $P(\tau_{\text{off}})$ for large (27 Å radius) and small (17 Å radius) QDs as well as for cases where the excitation intensity has been varied by nearly 3 orders of magnitude (0.1–100 kW/cm²).¹¹ In the case of CdSe/ZnS QDs, this inverse power law behavior in both $P(\tau_{\text{on}})$ and $P(\tau_{\text{off}})$ spans nearly seven decades in probability density and five decades in time. For InP QDs, the quality of the statistics is much more limited by photodegradation or “aging,” but log-log linearity in the off-time probability density spans nearly six decades in probability density and four decades in time. Similarly, the on-time probability density exhibits comparable log-log linearity spanning four decades in probability density and two decades in time. The shortest on/off events are currently limited by the 10 ms integration window; however, the strong log-log linearity of both on-time/off-time probability densities down to this time scale suggests that this inverse power law behavior might extend to even shorter times. Indeed, this prediction is confirmed by CdSe/ZnS QD experiments with a 50-fold reduction in an integration time bin from 10

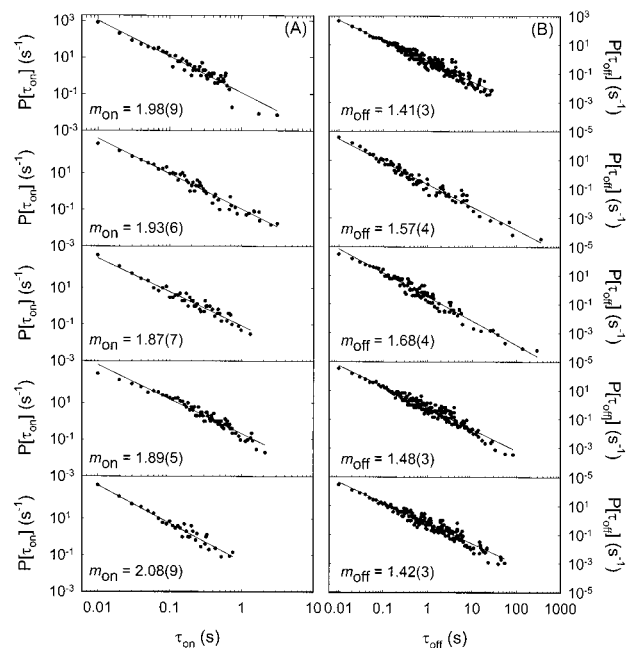


Figure 3. Log-log plots of the experimental on-time/off-time probability densities and accompanying linear fits for the five InP QDs shown in Figure 1. Column (A) shows log-log plots of $P(\tau_{\text{on}})$. Column (B) shows the accompanying off-time probability densities. In all cases, the slopes (errors) returned by the linear fitting procedure are shown below each trace. Average on-time and off-time slopes are $m_{\text{on}} = 2.0(2)$ and $m_{\text{off}} = 1.5(1)$.

ms to 200 μs, which show inverse power law behavior in both $P(\tau_{\text{on}})$ and $P(\tau_{\text{off}})$ down to at least the 10^{−4} s time scale.¹¹

Inverse power law blinking kinetics in $P(\tau_{\text{on}})$ and $P(\tau_{\text{off}})$ is verified in all 15 Å ($n = 28$) and 54 Å ($n = 5$) InP QDs investigated, and at all ranges of powers. By way of illustration, Figure 3 shows both on-time and off-time probability densities for five InP QDs at 0.24 kW/cm² laser excitation intensity, specifically those sampled by fluorescence trajectories shown in Figure 1. In all cases, both $P(\tau_{\text{on}})$ and $P(\tau_{\text{off}})$ exhibit quite linear log-log plots over many decades in probability density and in time. Results from a linear least-squares fit to the data are shown by solid lines, which also reveal slopes representing best estimates of the inverse power law exponents (m_{on} and m_{off}). Statistically, the on and off slopes are internally consistent for all QDs examined and, on average for the 5 QDs, yield $m_{\text{on}} = 1.9(1)$ and $m_{\text{off}} = 1.5(1)$, where the uncertainties represent one standard deviation. Similar power law exponent measurements have been made as a function of different dot size (15 to 54 Å) and laser intensity (100 to 390 nW); within experimental uncertainty, there is no evidence for sensitivity to these two parameters. However, it is worth noting that the least-squares fitted slopes do show significant variations ($\Delta m \approx 0.3$) from one InP dot to the next, especially for QDs from different synthetic batches. This range of InP power law exponents is in reasonable agreement with log-log data for 27 Å radius CdSe QDs. More specifically, the on-time exponents are roughly 10% higher for the range of InP vs CdSe QDs investigated [$m_{\text{on}} = 2.0(2)$ vs $m_{\text{on}} = 1.8(2)$], whereas the off-time exponents appear to be quite similar

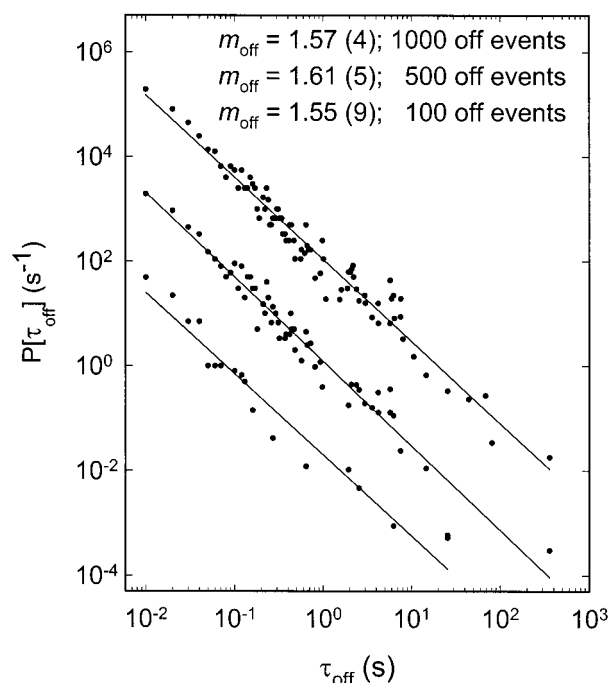


Figure 4. Plot of the off-time probability density, $P(\tau_{\text{off}})$, for successively smaller number of events composing the off-time distribution of a single 15 Å radius, InP QD. From top to bottom, the trajectories consist of 1000, 500, and 100 off events. Power law slopes at the top of the graph show no significant changes in m_{off} as a function of number of events.

[$m_{\text{on}} = 1.5(1)$ vs $m_{\text{on}} = 1.6(2)$]. The existence of such inverse power law kinetics for QDs of different sizes, composition, and surface modification suggests a common mechanism underlying fluorescence intermittency in each of these particles.

IV. Discussion

The presence of power law kinetics unambiguously rules out any *single* rate constant description for forward or reverse conversion between on/off manifolds. Indeed, in the perspective of a quantum jump model, such nonlinear semilogarithmic plots would require the forward/reverse rate constants to vary by 2 to 4 orders of magnitude over the course of an experiment. One scenario worth investigating, therefore, is whether such inverse power law behavior is consistent with a single exponential kinetic model, but with a slowly fluctuating rate constant due to time dependent local changes in the nanoenvironment. To address this, the fluorescence trajectories have been sequentially truncated by generating on-time and off-time probability densities from a progressively smaller fraction of the total on/off events. This is illustrated in Figure 4, where $P(\tau_{\text{off}})$ for a single InP QD consisting of ~ 1000 off events is truncated to the first 500 and 100 off events. In all cases, the linearity in $P(\tau_{\text{off}})$ is preserved down to the shortest 100-event trajectory. Furthermore, the value of the slope, m_{off} , obtained from the linear fitting procedure does not change within experimental error: 1000 events: $m_{\text{off}} = 1.57(4)$, 500 events: $m_{\text{off}} = 1.61(5)$, 100 events: $m_{\text{off}} = 1.55(9)$. This indicates that slow,

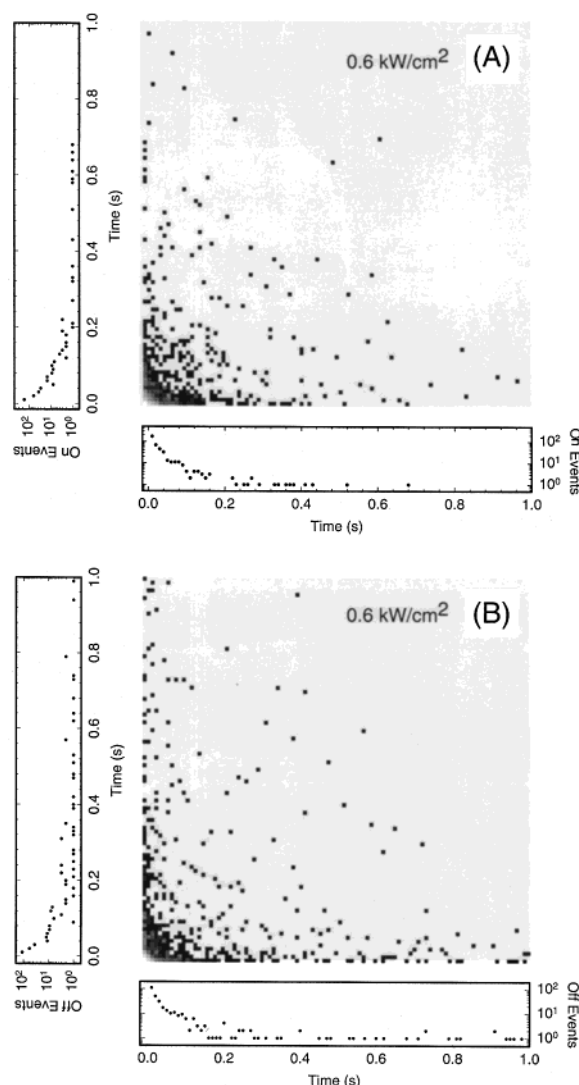


Figure 5. Correlation plots $G(\tau_{\text{on/off}}, \tau'_{\text{on/off}})$ of on-times versus successive on-times (A) and off-times followed by successive off-times (B). The sides of each box are 1 s and each pixel is a 10 ms intensity representation of the number of events common to both axes. A positive correlation would be indicated by a diagonal feature for the $\tau = \tau'$ axis, which is not seen in either the on or off distributions. Integrated projections of data along each axis are shown as semilogarithmic graphs.

large dynamic range fluctuations in a single-exponential $k_{\text{off} \rightarrow \text{on}}$ rate cannot be responsible for the observed inverse power law kinetics, at least for the off time distributions. The case is less definitive for the on-time power law kinetics (m_{on}); log–log analyses of successive “windows” of 100 on-events appear to indicate inverse power law slope variations of up to 30%. However, these fluctuations are also not inconsistent with 1σ variances between fluorescence trajectories for different dots from different size batches taken under identical excitation conditions.

Further dynamical restrictions on the time scale of such rate constant fluctuations can be obtained from correlation plots of on/off durations, as shown in Figure 5. For example, if these rate constant variations are very much slower than the time scale between on/off episodes, there should be a residual “memory” correlating the duration of successive on

(or off) episodes. This memory would manifest itself as a diagonal feature in a correlation plot of $G(\tau_{\text{on/off}}, \tau'_{\text{on/off}})$ along the $\tau_{\text{on/off}} = \tau'_{\text{on/off}}$ axis, where $\tau_{\text{on/off}}$ and $\tau'_{\text{on/off}}$ correspond to durations of adjacent events. No evidence for such a correlation is observed in any of the InP QDs investigated, which implies that fluctuations in the blinking rate constants must occur on time scales shorter than the “typical” duration of an on or off event. On the other hand, fluctuations very much faster than this would effectively lead to smearing over the spread of on/off rates, yielding single-exponential behavior with rate constants given by the average of the respective distributed rates. Thus, one arrives at the important conclusion that any fluctuations in the on/off rate constants must be occurring on a time scale comparable to the rate of blinking events.

Furthermore, due to the absence of a mathematically well-defined typical time for power law kinetics, this conclusion can be drawn even more tightly. The InP blinking data exhibit a 10^4 -fold dynamic range of typical time intervals (from 10 ms to 100 s), where the former is simply limited by the minimum integration time window and the latter reflects finite observation times due to photodegradation effects. One can reasonably argue that the only way fluctuations in these on/off rates can occur on a time scale comparable to (i.e., neither faster nor slower than) such an enormously broad range of observed time scales would be if the fluctuations are in fact synchronized with the on \rightarrow off or off \rightarrow on blinking event itself. This would be consistent, for example, with a model where each carrier ejection event causes changes in the local QD nanoenvironment, erasing any memory between successive blinking episodes. One example of this has been proposed by Neuhauser et al., whereby many electrons and holes are localized on the surface of the nanocrystallite surface due to accumulated photoionization events.¹² Ejection of electrons and holes to these surface states followed by their recombination could then allow for dynamic reorganization of the remaining carriers, providing a rationale for fluctuations in both charge and Coulomb fields imposed on the QD. Such models nicely bridge three experimental observations seen in isolated semiconductor QDs: fluorescence intermittency, charge blinking, and spectral diffusion.¹² In any case, the experimentally observed combination of (i) a power law distribution and (ii) the lack of correlation between adjacent $\tau_{\text{on/off}}$ episodes provides clear evidence for a significant change in the local QD environment synchronous with the blinking event.

At this point it is worth expanding the scope of discussion to include both InP and CdSe/ZnS QDs, and briefly consider possible physical mechanisms for the distributed kinetics and associated inverse power law behavior observed in both the on-time and off-time probability densities. A number of models have been proposed (quantum jumps, Auger ionization, Arrhenius or activated trapping/detrapping, tunneling to a distribution of states, and fluctuating barriers); physically all mechanisms entail photoionization of the quantum dot. In this respect it is assumed that an electron is ejected from the quantum dot, leaving it charged and nonemissive. This

proposition is supported by experiments that show light-induced charge blinking in isolated colloidal CdSe quantum dots and by recent theoretical efforts.^{27,28} What is not known, however, is where the ejected carrier resides, whether it is localized at “shallow” or “deep” surface states of the quantum dot, interface states in the core/shell structure, sites associated with the substrate, or in the surrounding polymer/glass matrix. It is also not known how the carrier leaves the quantum dot, whether it occurs through a tunneling mechanism, thermal ionization, by direct light induced ejection of the carrier, or by an Auger-assisted mechanism.

We first address what regions the carrier is likely to sample in order to be consistent with experimental observations of on/off blinking events occurring out to 10^3 s. For quantum tunneling through a square well barrier of height ΔV and width, d , tunneling rates can be estimated from the simple WKB expression,

$$\gamma_{\text{tun}} = A \exp(-2\sqrt{2m\Delta V}d/\hbar) \quad (2)$$

where the carrier attempt frequency A ($\approx 10^{14}$ – 10^{15} s⁻¹) reflects the maximum electron tunneling rate in the absence of any barrier. For a 1 eV barrier and a free electron mass, this expression corresponds to a 1/e decrease in probability per 0.976 Å in tunneling distance. Based on this, carrier tunneling lifetimes to/from trap states at the QD surface (note that for CdSe QDs, this requires tunneling through a ZnS overcoating) would occur well below μ s time scales, i.e., much too fast to be responsible for these slow blinking events. Indeed, short-lived blinking episodes may well be occurring involving these states on the submicrosecond time scale, but are much too fast to be resolved with our 10 ms experimental integration times. Thus, the data are not expected to be sensitive to the different electron–hole recombination dynamics on InP vs ZnS/CdSe QD passivation layers. (It is interesting to note in this regard that CdSe/ZnS studies with shorter (200 μ s) integration windows do show blinking and power law kinetic behavior. However, even this is too long for time scales of electron–hole pair recombination on QD surfaces.) To achieve sufficiently slow tunneling rates to rationalize the observed blinking rates, therefore, trap states extrinsic to the dot must be accessed. For example, based on a ≈ 4 eV barrier for tunneling through free space, events occurring on the 10^3 s time scale would involve tunneling to sites more than ≈ 20 Å away from the QD. Since no polymer matrix or glassy host is used in these experiments, one can speculate that the electron or ejected hole localizes itself on donor/acceptor-like states of the fused silica/glass microscope coverslip. This would also be qualitatively consistent with the strong dependence of fluorescence intensity on coverslip material; for example, we observe a 10-fold reduction in fluorescence intensity for CdSe/ZnS QDs on fused silica vs glass substrates.

Regardless of how the carrier is ejected from the quantum dot, the nonexponential power law kinetics appears to require a distribution of states to/from which the carrier tunnels. An additional subtle but crucial point is that a power law distribution is observed in both $P(\tau_{\text{on}})$ and $P(\tau_{\text{off}})$, which

allows one to convincingly infer that this distribution of states must be dynamic rather than static. The argument for this relies on simple kinetic principles: a static distribution of external trap states would translate into a static rate constant for carrier loss from the quantum dot, given by the sum over all rate constants to each site. As a result, any static model would necessarily predict a purely exponential distribution of on-time probability densities, which is fundamentally inconsistent with experimental observation.

Based on these observations, we can start to rule out a number of physical mechanisms by which the electron (or hole) leaves the quantum dot. The basic quantum jump model, which argues trapping of the carrier in a metastable shelf or intrinsic triplet-like state, cannot be responsible for the observed fluorescence intermittency. This is because associated with such a state would be two time independent rate constants for trapping and detrapping the carrier (in isolated single molecule studies, for example, these often correspond to intersystem crossing (ISC) and triplet quenching rates). The inverse power law kinetics for both $P(\tau_{\text{on}})$ and $P(\tau_{\text{off}})$ requires that such rates be highly distributed in time. Furthermore, the μs to minute time scale of events is inconsistent with the intrinsic lifetime of QD electronic states.²⁸ For an Auger ejection mechanism, a quadratic dependence of the ejection rate with excitation intensity is predicted. Experiments have been conducted exciting CdSe QDs (ZnS or CdS overcoated) both at the band edge and further to the blue into a dense manifold of states;^{7–12} in all cases, no such quadratic dependence of the on to off rate has been observed. Rather, it is generally observed to follow a linear dependence on intensity.^{7,27} This argues against a direct “over the barrier” Auger ionization but does not rule out an Auger-assisted tunneling mechanism.

Experiments on CdSe/ZnS QDs show little or no temperature dependence to the blinking power law statistics.^{10,29} This lack of temperature dependence argues against any activated or Arrhenius mechanism coupled to a static distribution of trap states intrinsic to the quantum dot. The special case of trap sites with exponentially distributed trap depths represents a particularly interesting possibility at first, since such a model rigorously predicts an inverse power law in $P(\tau_{\text{off}})$.³⁰ However, this model also predicts a modest temperature dependence of the form $m = 1 + \alpha kT$, where α is a temperature independent coefficient related to the trap state distribution.¹¹ Furthermore, the number of surface/interface states required to be consistent with such a dynamic range of inverse power law behavior would be on the order of several hundred to several thousand, i.e., comparable to or greater than the total number of In and P sites available [15 Å radius InP ~ 200 sites, 27 Å radius InP ~ 1000 sites].³¹ This would be inconsistent with the relatively high quantum yields reported for HF etched InP particles (up to 30% at room temperature) and of ZnS overcoated CdSe QDs (up to 50% at room temperature), since in effect the surface would consist entirely of trap states that render the particle nonemissive. Finally, any static distribution of trap sites is fundamentally inconsistent with an inverse power law behavior in the on-time probability density, as argued above.

It is also interesting to note that simple bulk electron affinity based estimates of barrier heights in InP (3.70 eV) vs CdSe (4.59 eV) would predict larger ($\approx 11\%$) 1/e tunneling distances for InP, which is roughly consistent with the observed ratio of on-time exponents for the two QD materials.

One plausible (albeit phenomenological) model consistent with current data is via quantum tunneling (possibly Auger assisted) of the carrier through a barrier, but where modest ($\approx \pm 25\%$) fluctuations in this barrier height or width translate into tunneling rates that fluctuate in time over 10^5 -fold. The importance of carrier tunneling is already evidenced by the observed red shift of the QD absorption upon overcoating CdSe QDs with ZnS (or CdS).^{24–26} As noted above, the location of these trap sites is argued to be extrinsic to the QD in order to observe on/off events on experimentally accessible time scales. While the explicit nature of these trap states is not clear, they would most likely involve substrate states in the fused silica or glass coverslip. Furthermore, to obtain the observed dynamic range of inverse power law behavior in both $P(\tau_{\text{on}})$ and $P(\tau_{\text{off}})$, the model requires 10^5 -fold fluctuations in tunneling rates to/from an isolated trap state, presumably due to changes in the local environment of the quantum dot. As one explicit physical picture, such fluctuations could arise from conformational changes in the organic ligands passivating the surface of the colloidal particles, which, in turn, modulates the conductivity for carrier transport between isolated trap states and the QD. This model also has the advantage that it would predict the greatest dynamic range of tunneling rate fluctuations in the limit of only very few trap states, which is therefore more likely to be consistent with the high quantum yield and crystallinity of ZnS overcoated CdSe and HF etched InP QDs. Alternatively, one could argue for the dynamic reorganization of multiple charges decorating the quantum dot as a means of varying the local nanoenvironment of the particle for the long-range tunneling events. This is consistent with the model proposed by Bawendi and co-workers¹² for blinking and spectral diffusion, but would still require that long time scale tunneling rates measured in these experiments correspond to carrier recombination events originating from distances far from the QD. The specific kinetic implications of these and other possible models for quantum dot fluorescence intermittency have been investigated and will be discussed elsewhere in more detail.³²

V. Summary and Conclusions

The present work complements the knowledge base on fluorescence intermittency by providing additional kinetic studies of blinking in systems other than ZnS overcoated CdSe QDs. In this respect, the observation of inverse power law blinking kinetics in III–V InP colloidal semiconductor QDs supports our working hypothesis that local environmental fluctuations profoundly influence carrier photoionization and recovery rates underlying the on/off fluorescence intermittency. In addition, a growing body of evidence, from

the correlation between spectral diffusion and blinking to the remarkable coincidence of blinking time scales needed to achieve an inverse power law yet show no correlation between subsequent on/off times, points to the likelihood that these carrier ejection/recombination events themselves initiate changes in the QD nanoenvironment. As a consequence, a more detailed understanding of this inverse power law behavior may enable better insight into important chemical kinetic and dynamic processes involving these QDs, which in turn may enable successful implementation of these novel materials in future optoelectronic devices.

Acknowledgment. We would like to acknowledge the National Science Foundation, and the National Institute of Standards and Technology for research support. M.K. would like to thank the National Research Council for a postdoctoral fellowship. O.I.M. and A.J.M. would like to thank the U.S. Department of Energy, Office of Science, Division of Chemical Sciences for financial support.

References

- (1) Dickson, R. M.; Cubitt, A. B.; Tsien, R. Y.; Moerner, W. E. *J. Phys. Chem. A* **1997**, *388*, 355. Peterman, E. J.; Brasselet, S.; Moerner, W. E. *J. Phys. Chem. A* **1999**, *103*, 10553.
- (2) Bopp, M. A.; Jia, Y.; Li, L.; Cogdell, R.; Hochstrasser, R. M. *Proc. Natl. Acad. Sci. U.S.A.* **1997**, *94*, 10630.
- (3) Vanden Bout, D.; Yip, W. T.; Hu, D.; Fu, D. K.; Swager, T. M.; Barbara, P. F. *Science* **1997**, *277*, 1074.
- (4) Mason, M. D.; Credo, G. M.; Weston, K. D.; Buratto, S. K. *Phys. Rev. Lett.* **1998**, *80*, 5405.
- (5) Sugisaki, M.; Ren, H. W.; Nair, S. V.; Lee, J. S.; Sugou, S.; Okuno, T.; Masumoto, Y. *J. Lumin.* **2000**, *15*, 40. Sugisaki, M.; Ren, H. W.; Nishi, K.; Masumoto, Y. *Phys. Rev. Lett.* **2001**, *86*, 4883.
- (6) Pistol, M. E.; Castrillo, P.; Hessman, D.; Prieto, J. A.; Samuelson, L. *Phys. Rev. B* **1999**, *59*, 10725.
- (7) Nirmal, M.; Dabbousi, B. O.; Bawendi, M. G.; Macklin, J. J.; Trautman, J. K.; Harris, T. D.; Brus, L. E. *Nature* **1996**, *383*, 802.
- (8) Tittel, J.; Gohde, W.; Koberling, F.; Mews, A.; Kornowski, A.; Weller, H.; Eychmuller, A.; Basche, Th. *Ber Bunsen-Ges. Phys. Chem.* **1997**, *101*, 1626.
- (9) Banin, U.; Bruchez, M.; Alivisatos, A. P.; Ha, T.; Weiss, S.; Chemla, D. S. *J. Chem. Phys.* **1999**, *110*, 1195.
- (10) Kuno, M.; Fromm, D. P.; Hamann, H. F.; Gallagher, A.; Nesbitt, D. *J. J. Chem. Phys.* **2000**, *112*, 3117.
- (11) Kuno, M.; Fromm, D. P.; Hamann, H. F.; Gallagher, A.; Nesbitt, D. *J. J. Chem. Phys.* **2001**, *115*, 1028.
- (12) Neuhauser, R. G.; Shimizu, K.; Woo, W. K.; Empedocles, S. A.; Bawendi, M. G. *Phys. Rev. Lett.* **2000**, *85*, 3301.
- (13) Rodrigues-Herzog, R.; Trotta, F.; Bill, H.; Segura, J. M.; Hecht, B.; Guntherodt, H. J. *Phys. Rev. B* **2000**, *62*, 11163.
- (14) Barnes, M. D.; Mehta, A.; Thundat, T.; Bhargava, R. N.; Chabra, V.; Kulkarni, B. *J. Phys. Chem. B* **2000**, *104*, 6099.
- (15) Lu, H. P.; Xie, X. S. *Nature* **1997**, *385*, 143.
- (16) Ha, T.; Enderle, Th.; Chemla, D. S.; Selvin, P. R.; Weiss, S. *Chem. Phys. Lett.* **1997**, *271*, 1.
- (17) Weston, K. D.; Carson, P. J.; Metiu, H.; Buratto, S. K. *J. Chem. Phys.* **1998**, *109*, 7474.
- (18) Cook, R. J.; Kimble, H. J. *Phys. Rev. Lett.* **1985**, *54*, 1023.
- (19) Nagourney, W.; Sandberg, J.; Dehmelt, H. *Phys. Rev. Lett.* **1986**, *56*, 2797. Bergquist, J. C.; Hulet, R. G.; Itano, W. M.; Wineland, D. *J. Phys. Rev. Lett.* **1986**, *57*, 1699. Sauter, Th.; Neuhauser, W.; Blatt, R.; Toschek, P. E. *Phys. Rev. Lett.* **1986**, *57*, 1696.
- (20) Basche, Th.; Kummer, S.; Brauchle, C. *Nature* **1995**, *373*, 132.
- (21) Kulzer, F.; Koberling, F.; Christ, Th.; Mews, A.; Basche, Th. *Chem. Phys.* **1999**, *247*, 23.
- (22) Lacoste, Th. D.; Michalet, X.; Pinaud, F.; Chemla, D. S.; Alivisatos, A. P.; Weiss, S. *Proc. Nat. Acad. Sci. U.S.A.* **2000**, *97*, 9461. van Sark, W. G. J. H. M.; Frederix, P. L. T. M.; van den Heuvel, D. J.; Asselbergs, M. A. H.; Senf, I.; Gerritsen, H. C. *Single Mol.* **2000**, *1*, 291.
- (23) Micic, O. I.; Cheong, H. M.; Fu, H.; Zunger, A.; Sprague, J. R.; Mascarenhas, A.; Nozik, A. J. *J. Phys. Chem. B* **1997**, *101*, 4904.
- (24) Peng, X. G.; Schlamp, M. C.; Kadavanich, A. V.; Alivisatos, A. P. *J. Am. Chem. Soc.* **1997**, *119*, 7019.
- (25) Dabbousi, B. O.; Viejo, J. R.; Mikulec, F. V.; Heine, J. R.; Mattoussi, H.; Ober, R.; Jensen, K. F.; Bawendi, M. G. *J. Phys. Chem. B* **1997**, *101*, 9463.
- (26) Hines, M. A.; Guyot-Sionnest, P. *J. Phys. Chem.* **1996**, *100*, 468.
- (27) Krauss, T. D.; Brus, L. E. *Phys. Rev. Lett.* **1999**, *83*, 4840. Krauss, T. D.; O'Brien, S.; Brus, L. E. *J. Phys. Chem. B* **2001**, *105*, 1725.
- (28) Efros, A. L.; Rosen, M. *Phys. Rev. Lett.* **1997**, *78*, 1110.
- (29) Shimizu, K. T.; Neuhauser, R. G.; Leatherdale, C. A.; Empedocles, S. A.; Woo, W. J.; Bawendi, M. G. *Phys. Rev. B* **2001**, *63*, 5316.
- (30) Randall, J. T.; Wilkins, M. H. F. *Proc. R. Soc. London* **1945**, *184*, 366.
- (31) For this calculation, a lattice parameter of 5.87 Å is assumed. The unit cell volume is therefore taken to be 202 Å³.
- (32) Kuno, M.; Fromm, D. P.; Johnson, S. T.; Gallagher, A.; Nesbitt, D. J. (manuscript in preparation).

NL010049I